JOURNAL OF CATALYSIS 131, 94–103 (1991)

Transient Diffusion, Sorption, and Desorption of Cyclopropane in NaX Zeolite

ANGELOS M. EFSTATHIOU,* STEVEN L. SUIB,*,†,[1] AND CARROLL O. BENNETT*

*Department of Chemical Engineering and †Department of Chemistry, University of Connecticut, Storrs, Connecticut 06269-3060

Received January 30, 1991; revised April 15, 1991

Transient diffusion, sorption, and desorption experiments of cyclopropane in NaX zeolite at 1 bar in a flow microreactor reveal that the nature of the diluent gas used in the sorbate mixture affects the kinetics of intracrystalline mass transport of cyclopropane in the zeolite. The rate of intracrystalline mass transport and the equilibrium uptake are strongly dependent on temperature. The outward mass transport of cyclopropane into 1 bar Ar gas is found to be an activated process with an apparent activation energy of 7.4 kcal/mol. Rates of diffusion are affected by the gas phase pressure. The enthalpy of sorption for cyclopropane at loadings approaching zero is found to be −9.0 kcal/mol, and the entropy of sorption is −18.2 cal/mol-K.

INTRODUCTION

Transient methods in flow reactors have been used mainly to study reactions on Group VIII metal-supported catalysts (*1–7*). These methods have proven useful for the measurement of the reactivities and *in situ* surface coverage of intermediates (*3–7*). Transient responses controlled by the dynamics of surface reactions in supported metal systems (i.e., Al_2O_3, SiO_2) are obtained by designing experiments so as to minimize inter- and intraparticle mass transport resistances. In metal zeolite systems, however, effects depend on the intracrystalline diffusion of reactants and/or products cannot be eliminated by reducing the crystallite size (*8*).

The objective of the present work was to study the diffusion and sorption processes of cyclopropane (c-C_3H_6) in NaX zeolite. The sorption of c-C_3H_6 in a variety of diluent gases has been probed. Desorption under temperature-programmed (TPD) and isothermal conditions has been carried out. Diffusivities of c-C_3H_6 have been measured. The enthalpy and entropy of sorption of c-C_3H_6 have been calculated based on appropriate experimental conditions and use of a Langmuir isotherm. The investigation of transient responses plays an important role in the present work.

The present studies are relevant to future investigation of the cyclopropane/hydrogen reaction in NaX zeolites containing a catalytically active metal (*9*). We have already investigated the diffusion and sorption of hydrogen in NaX at 1 bar (*10*). Specific results from that work showed that uptake and diffusivity of molecular hydrogen were markedly influenced by cation type in the zeolite (*10*).

EXPERIMENTAL

Catalyst. Linde NaX and NaA zeolites were purchased from Alfa Ventron Corp., Danvers, MA and used without further purification. The crystal size of both zeolites was about 1.2 μm as determined by scanning electron microscopy. Dehydration and loading of the zeolite into the reactor under inert atmosphere were done by procedures previously described (*10*). Prior to transient diffusion and sorption studies, the sample was checked *in situ* for residual H_2O by mass spectrometry. The zeolite bed was sup-

[1] To whom correspondence should be addressed.

0021-9517/91 $3.00

ported by fine stainless-steel screens and glass wool.

Reactor-flow system. A once-through stainless-steel microreactor (0.75 mL) was used in this study. Response experiments have shown that the reactor behaves as an ideal mixed-flow reactor or continuously stirred tank reactor (CSTR) (*4, 5*). The flow system was the same as described earlier (*5*). All the lines and valves after the reactor (including the inlet capillary and ion source of the mass spectrometer) were heated at 150°C to avoid possible adsorption of cyclopropane. The pure time delay (6 s at 30 mL/min) of c-C_3H_6 was obtained by measuring the forcing function (*5*) by using a bypass around the reactor. A data system was used to subtract this time delay from the time response of c-C_3H_6 obtained after the sorbate mixture was passed through the reactor loaded with zeolite. Step changes in the feed and temperature-programmed desorption (TPD) experiments that were used have been described previously (*4, 5, 10*).

Mass spectrometry. The high-resolution mass spectrometer (Nuclide 12-90-G), data acquisition, calibration, and integration of the mass spectrometer response have been described (*4*). Cyclopropane, Ar, and H_2O were monitored at m/e = 42, 40, and 18, respectively.

Gas mixtures. Transient sorption studies at 1 bar total pressure were performed with dilute mixtures of 0.5 mol% (3.8 Torr) c-C_3H_6 in three different diluent gases: H_2, He and Ar. Various other c-C_3H_6/H_2 mixtures in the range 2–300 Torr of c-C_3H_6 were also used in this work. Cyclopropane was CP grade (Matheson Co.), and Ar, He, and H_2 were zero grade (Aero All-Gas Co). Less than 2 ppm of propylene was measured by gas chromatography in the 0.5 mol% sorbate mixtures. Argon was used as carrier gas in the temperature-programmed desorption studies. Purification of this gas has been described (*5*). The flow rate of all gases used was 30 mL/min (ambient).

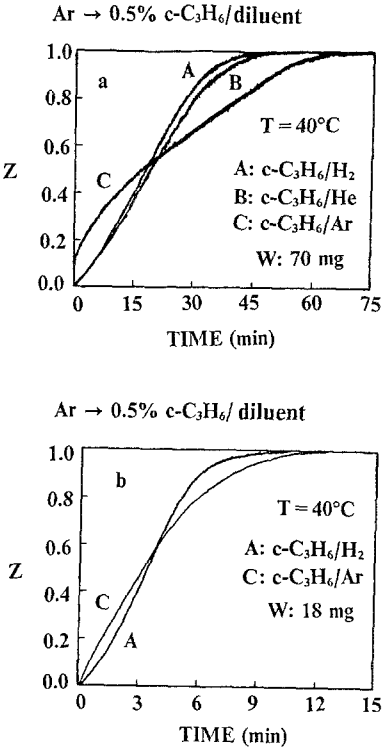

FIG. 1. Effect of diluent gas on the dimensionless gas phase transient response (Z) of c-C_3H_6 in Na*X*. Delivery sequence: Ar → c-C_3H_6/diluent; T = 40°C; diluent gas: H_2, He, Ar. (a) 70 mg sample, (b) 18-mg sample.

RESULTS

(*A*) *Transient Diffusion and Sorption of Cyclopropane*

Transient sorption responses of c-C_3H_6 in dehydrated Na*X* zeolite (70 mg) for three different diluent gases (H_2, He, and Ar) are shown in Fig. 1a. The ordinate is labeled Z, which repesents the concentration (mol%) of c-C_3H_6 in the gas phase at some time t, $y(t)$, divided by the gas phase concentration of c-C_3H_6 at equilibrium time, y_∞, or

$$Z(t) = y(t)/y_\infty. \qquad (1)$$

These data show that the gas phase concentration of c-C_3H_6 rises faster (small sorption rate) when Ar diluent gas is used instead of H_2 or He. Results for the mixing curve of CSTR microreactor and for Na*A* zeolite are

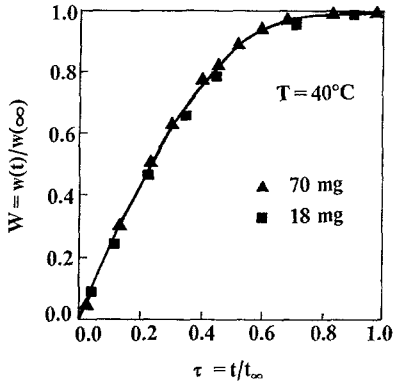

FIG. 2. Dimensionless transient uptake, W, of c-C_3H_6 in NaX based on results of Fig. 1, curve A.

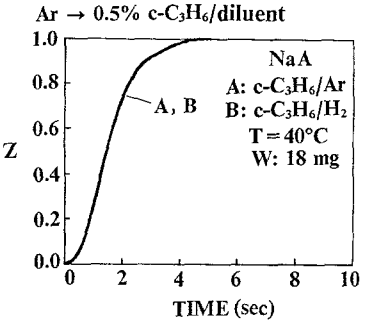

FIG. 3. Effect of diluent gas on the dimensionless gas phase transient response (Z) of c-C_3H_6 in NaA. Delivery sequence: Ar → c-C_3H_6/diluent; T = 40°C; diluent gas: H_2, Ar; 18 mg sample.

given below for comparison and to compensate the data for NaX.

Similar data for H_2 and Ar diluent gases are given in Fig. 1b for an 18-mg sample. The gas phase rate of concentration rise of c-C_3H_6 is again initially greater for Ar than for H_2. Both samples show equilibrium values (Z = 1) at long times, after about 45 min for the sample of Fig. 1a (curve A) and after about 10 min for the sample of Fig. 1b (curve A). From the results of Fig. 1 the same equilibrium uptake (1.4 mmol/g, Z = 1) is obtained independent of the diluent gas used.

Data for the gas phase response of c-C_3H_6 with H_2 diluent gas have been used to determine the amount of c-C_3H_6 sorbed in the NaX samples. The ratios of the amount (mmol/g) of c-C_3H_6 sorbed at some time t, $[w(t)]$, divided by the amount sorbed at equilibrium, $[w(\infty)]$, as a function of normalized time τ for both samples of Fig. 1 are shown in Fig. 2 for sorption of c-C_3H_6 at 40°C; τ = (t/time to reach equilibrium). These data show that at a given fractional time τ the same fractional uptake W is obtained regardless of the amount of sample used.

To probe the effect of diluent gas on the transient responses of c-C_3H_6 in Fig. 1, the experiments of Fig. 1b were repeated with an 18-mg NaA (4A) sample. The results obtained given in Fig. 3 clearly show that the transient response of c-C_3H_6 is independent of the diluent gas used. In addition, there is practically no uptake of c-C_3H_6 and the curves A and B are the same as the mixing curve of the CSTR microreactor (*3, 5*). This behavior is discussed later.

The effect of flow rate on the sorption of c-C_3H_6 in H_2 diluent is shown in Fig. 4 for flow rates varying from 0.34 to 0.75 cm^3/s. Equilibrium (Z = 1) is reached first for the fastest flow rate, after about 6 min.

Transient sorption responses of c-C_3H_6 at elevated temperatures like 120 and 160°C, which have previously been used for cata-

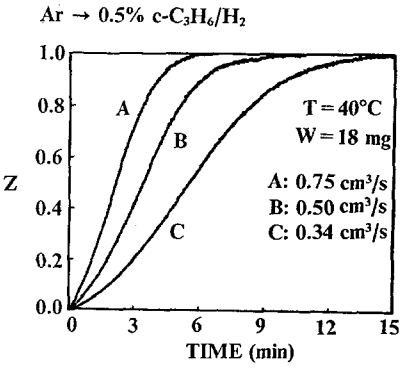

FIG. 4. Effect of flow rate q (cm^3/s) on the dimensionless gas phase transient response (Z) of c-C_3H_6 in NaX. Delivery sequence: Ar → c-C_3H_6/H_2. T = 40°C; 18 mg NaX. Curve A, 0.75 cm^3/s; curve B, 0.50 cm^3/s; curve C, 0.34 cm^3/s.

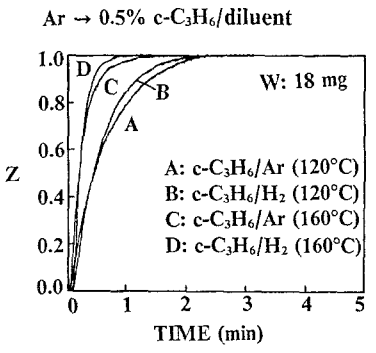

FIG. 5. Effect of temperature on the dimensionless gas phase transient response (Z) of c-C_3H_6 in NaX. Delivery sequence: Ar → c-C_3H_6/diluent, T; diluent gas: H_2, Ar; 18 mg NaX.

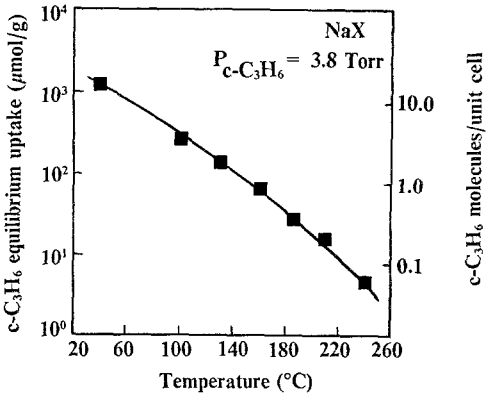

FIG. 7. Equilibrium uptake of c-C_3H_6 (μmol/g, molecules/unit cell) vs temperature for NaX. $P_{c\text{-}C_3H_6}$ = 3.8 Torr (0.5 mol%).

lytic reactions (*9*), are shown in Fig. 5 for both Ar and H_2 diluent gases. A similar diluent gas effect occurs as observed in Fig. 1, but the effect is less pronounced. In addition, equilibrium is reached more rapidly for the 160°C experiments than for those done at 120°C.

Experiments similar to those of Fig. 5 have been done for a range of temperatures between 160 and 240°C for H_2 diluent gas as shown in Fig. 6. There is a progressively faster approach to equilibrium as the temperature is increased. The mixing curve (curve A) of Fig. 6 shows the response of the system to a nonsorbing gas when the switch from He to 1% Ar/He is made through the reactor loaded with NaX zeolite.

Equilibrium uptake data of c-C_3H_6 as a function of temperature can be extracted from Figs. 1, 5, and 6 and these are plotted in Fig. 7. Note that the equilibrium uptake of c-C_3H_6 is plotted on a log scale and that this isobar is for a pressure of 3.8 Torr.

Figure 8 shows equilibrium uptake data at 40 and 100°C for c-C_3H_6 pressures in the

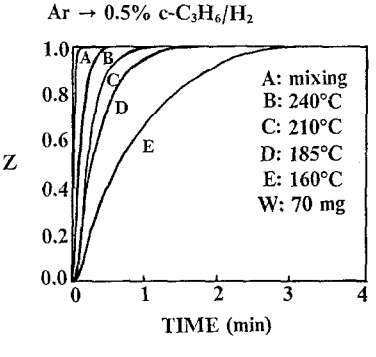

FIG. 6. Effect of temperature on the dimensionless gas phase transient response (Z) of c-C_3H_6 in NaX. Delivery sequence: Ar → c-C_3H_6/H_2, T; 70 mg NaX. Curve A is the mixing curve at 160°C of the CSTR microreactor.

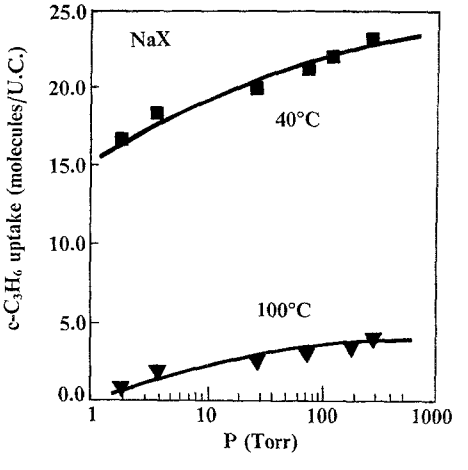

FIG. 8. Equilibrium c-C_3H_6 sorption isotherms at 40 and 100°C for NaX zeolite.

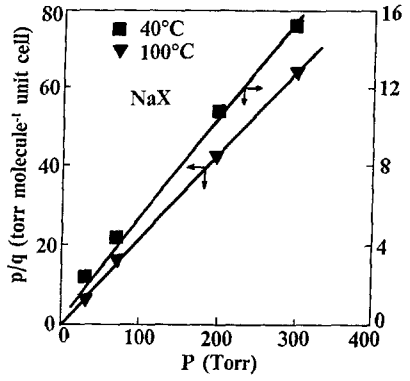

FIG. 9. Analysis of c-C_3H_6 equilibrium uptake data of Fig. 8 based on Langmuir isotherm for sorption.

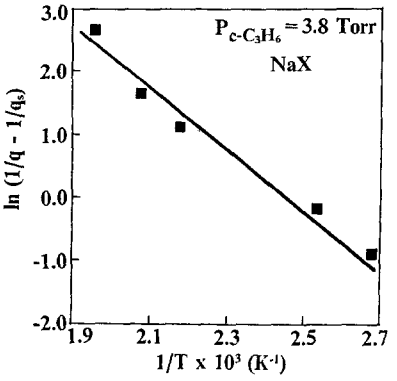

FIG. 10. Determination of limiting values for enthalpy (ΔH^0) and entropy (ΔS^0) of sorption for c-C_3H_6 in NaX at 3.8 Torr.

range 2–300 torr. The equilibrium data of Fig. 8 in the range 30–300 torr were analyzed using the Langmuir isotherm. The appropriate equation (*8*) can be rearranged to give

$$P/q = 1/bq_s + P/q_s, \qquad (2)$$

where q is the c-C_3H_6 uptake (molecule/u.c.), q_s is the c-C_3H_6 uptake at saturation (molecule/u.c.), b is the Langmuir equilibrium constant (Torr^{-1}), and P is the pressure of c-C_3H_6 (Torr). Figure 9 shows the results obtained after using the data of Fig. 8 and Eq. (2). A good fit to a Langmuir isotherm is apparent from which are obtained q_s = 23.9 and 4.1 (molecule/u.c.) for the temperatures of 40 and 100°C, respectively, and b = 0.135 and 0.045 (Torr^{-1}) for the same temperatures.

Thermodynamic data can be extracted from the isobar of Fig. 7 based on a Langmuir isotherm for sorption. The appropriate equation (*8*) can be rearranged to give

$$\ln(1/q - 1/q_s) = \ln(1/b_0 q_s P) + \Delta H^0/\mathrm{RT}, \qquad (3)$$

where $b_0 = \exp(\Delta S^0/R)$, ΔS^0 is the entropy of sorption (cal/mol-K), and ΔH^0 is the heat of sorption (kcal/mol).

Figure 10 gives the results obtained after using Eq. (3) and the data of Fig. 7 in the range 100–240°C. A value of 23.9 (molecule/u.c.) is used for q_s as obtained from the isotherm at 40°C in Fig. 8. The enthalpy of sorption of c-C_3H_6 (ΔH^0) is found to be −9.0 kcal/mol, and the entropy of sorption (ΔS^0) is −18.2 cal/mol-K. Values of q_s higher than that used do not affect the results by more than 10%.

The gas phase transients of Fig. 4 (curves A, C) are compared to the gas phase transient response that would be observed if an equilibrium between the gas and sorbed phase of c-C_3H_6 is assumed for the same experimental conditions. The mathematical treatment for obtaining this equilibrium gas phase response is given in the Appendix. Figure 11 gives the gas phase transient re-

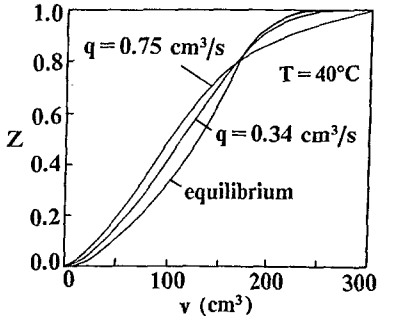

FIG. 11. Simulated gas phase dimensionless transient response of c-C_3H_6 for the case where equilibrium according to the Langmuir isotherm between the gas and sorbed phase of c-C_3H_6 is assumed. For comparison, experimental results from Fig. 4 are also given.

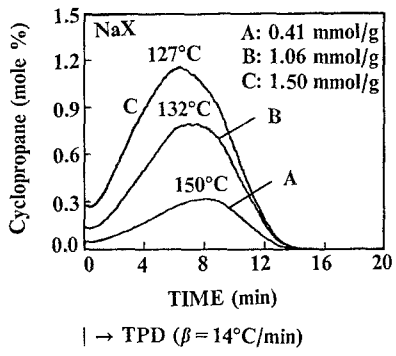

FIG. 12. TPD experiments for measuring c-C_3H_6 sorption in NaX. Experimental procedure: 3.8 Torr c-C_3H_6/H_2 (40°C, Δt, θ_i) → Ar (90 s), 40°C → TPD (β = 14°C/min); 70 mg NaX. Curve A: Δt = 5 min, θ_i = 0.41 mmol/g; Curve B: Δt = 15 min, θ_i = 1.06 mmol/g; Curve C: Δt = 45 min, θ_i = 1.50 mmol/g. The effect of θ_i on the peak maximum temperature T_m is also shown.

sponses of c-C_3H_6 for two flow rates (curves A and C of Fig. 4) and the simulated response based on equilibrium conditions. Here the results are plotted as Z vs v, where $v = qt$. From these results it can be seen that the lower the flow rate q the closer to equilibrium the response is. Note that the area between a given curve in Fig. 11 and that of mixing curve (curve A, Fig. 6) provide the total amount sorbed. The equilibrium response in Fig. 11 provides 1.65 mmol/g compared to 1.4 mmol/g (Fig. 1). This difference probably arises because the Langmuir isotherm does not perfectly fit the actual equilibrium data in the range of 0–3.8 Torr of c-C_3H_6 for the experiments of Fig. 4.

(*B*) *Transient Desorption Studies*

Temperature-programmed desorption data for c-C_3H_6 sorbed at 40°C and 3.8 Torr for coverages ranging from 0.41 to 1.50 mmol/g are shown in Fig. 12. For the experiment at the lowest coverage (Fig. 12, curve A) the maximum temperature (T_m) of the TPD is 150°C, which is the highest T_m of all the different coverages.

The kinetic parameters D_0 and E associated with the diffusivity D ($D = D_0 \exp(-E/RT)$) can be obtained from results similar to those of Fig. 12 in a manner previously described (*10*). For sorption at 40°C, 15 min, and 3.8 Torr of c-C_3H_6, by varying the heating rate β between 10 and 20°C/min, values of E = 7.4 kcal/mol and $D_0/r^2 = 2.2$ s^{-1} are obtained. Using r = 0.6 μm, where r is the radius of a spherical zeolite crystal, values of $D_0 = 3.6 \times 10^{-9}$ cm^2/s and $D = 2.4 \times 10^{-14}$ cm^2/s for T = 40°C are obtained.

TPD experiments similar to those of Fig. 12 were done at 70 Torr of c-C_3H_6 sorption pressure after 5 and 45 min of sorption. Transient gas phase concentrations of c-C_3H_6 at these higher partial pressures cannot be measured during sorption since the gas phase concentrations are out of the linear range of the mass spectrometer detector. There is little difference in the amount of c-C_3H_6 sorbed for these two conditions, 1.45 mmol/g for 5 min and 1.61 mmol/g for 45 min. The T_m for both experiments is also found to be the same (125°C).

Isothermal desorption data in H_2 carrier gas for NaX that had sorbed an equilibrium amount of c-C_3H_6 from 3.8 Torr c-C_3H_6 in H_2 at 100, 120, and 160°C are given in Fig. 13. The mole percent of c-C_3H_6 at equilibrium is 0.5 and decreases exponentially with time for each isothermal desorption. The isothermal desorption of c-C_3H_6 at 100°C

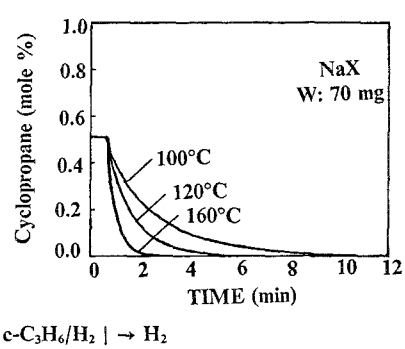

FIG. 13. Transient isothermal outward diffusion of c-C_3H_6 into 1 bar H_2 gas. Delivery sequence: Ar → c-C_3H_6/H_2 (T) until equilibrium is reached → H_2; 70 mg NaX; T = 100, 120, 160°C.

occurs in 10 min, whereas at 160°C it occurs in 3 min.

DISCUSSION

(A) *Transient Diffusion and Sorption of Cyclopropane*

An effect of diluent gas on the rate of diffusion of c-C_3H_6 in Na*X* is apparent. The data of Figs. 1 and 5 show that the initial sorption rate of c-C_3H_6 is greater with the diluents H_2 and He than with Ar. This is true for a 70-mg Na*X* sample (Fig. 1a) and for an 18-mg Na*X* sample (Fig. 1b). The normalized equilibrium uptake data for c-C_3H_6 (Fig. 2) show similar results for both catalyst beds.

These data suggest that heat and mass transfer resistances outside the zeolite crystallites have been minimized and that the same sorption rates for both samples are obtained. Therefore, the sorption and desorption data presented here represent phenomena related to the microstructure of the zeolite.

The results of Fig. 3 with Na*A* help to clarify the diluent gas effect observed in Figs. 1 and 5. The Na*A* zeolite has about a 4.0-Å apparent pore opening. The complete exclusion of c-C_3H_6 with a 4.2-Å kinetic diameter is, therefore, to be expected. Scanning electron micrographs for the Na*X* and Na*A* used (both 600 mesh) showed about the same crystal size and intercrystalline structure. In Fig. 3 the measured time to obtain $Z = 1.0$ for the c-C_3H_6 is fast (5 s for completion) and unaffected by the nature of diluent gas. It is also the same as the mixing curve obtained for the replacement of one of the diluent gases by another. In Fig. 1 the time to reach $Z = 1.0$ does depend on the nature of the diluent gas. It is clear, therefore, from the results of Fig. 3 that the transient mass transport of c-C_3H_6 into Na*X* is controlled by intracrystalline diffusion processes only.

The differences in diffusion and sorption in the presence of different diluent gases are difficult to quantify at this point. It is suggested that these differences are due to collisional effects that influence the diffusion mechanism of c-C_3H_6 from one cavity to the next one, rather than to a competition for sites between the inert diluent gases and c-C_3H_6. It is logical to think that the larger size of Ar compared to H_2 or He would impose a greater difficulty for c-C_3H_6 to pass through the window between adjacent supercages (α cages) of Na*X*. Note that the amount of Ar or He sorbed in Na*A* (*13*, *14*) at 40°C is at least 3 orders of magnitude lower than the amount of c-C_3H_6 sorbed as found here (Fig. 1). Large differences in the amount of Ar or He sorbed in Na*X* with respect to Na*A* are not expected. The amount of H_2 sorbed in Na*X* is also found to be very small (2 μmol/g) (*10*).

Further evidence for a diluent effect can be found in the work of Kärger *et al.* (*15*) who have observed by NMR a decrease in the self-diffusion of cyclohexene in Na*X* when Ar was present in the zeolite cavities.

The effect of Ar diluent gas on the intracrystalline transient mass transport of c-C_3H_6 diminishes with increasing sorption temperature (Figs. 1, 5). This might be due to an increase in the effective opening through which c-C_3H_6 passes toward the sorption sites, with increasing temperature. Thus, at temperatures like 160°C the rate of diffusion of c-C_3H_6 is little influenced by whether H_2, He, or Ar diluent gas is present inside the zeolite cavities.

The equilibrium data of Fig. 7 for Na*X* suggest that the concentration of c-C_3H_6 in the cavities may influence the selectivity of reactions between c-C_3H_6 and H_2. The number of molecules of c-C_3H_6 per unit cell is significantly decreased from about 20 at room temperature to less than 1 at 220°C. A similar behavior has also been obtained with NaY and Ru/NaY catalysts (*16*). Even though the c-C_3H_6/H_2 reaction on Co/Na*X* (*9*) and Ru/Ca*A* (*25*) was suggested to be a structure-sensitive reaction, care must be given to decouple the effects of temperature and particle size on the aforementioned reaction with metal-loaded zeolite systems.

Note that agglomeration of small cobalt particles (5 Å) present in the cavities of NaX readily occurs at temperatures higher than 150°C (*9*).

The thermodynamic parameters ΔH^0 and ΔS^0, −9.0 kcal/mol and −18.2 cal/mol-K, respectively of Fig. 10 for c-C_3H_6 are in line with published calorimetric data for propane (*11*), a sorbate molecule similar to c-C_3H_6. It should be noted that the good fit to the Langmuir isotherm for the conditions of Fig. 10 should not imply that the sorbate layer of c-C_3H_6 is immobile, or that the sites in NaX are energetically homogeneous. Similar results to those of Fig. 10 have been reported (*8*). Various other isotherms could be used to fit the data of Figs. 7 and 8 (*8*). However, the Langmuir isotherm provided reasonable values for ΔH^0 and ΔS^0, and a detailed investigation of the results of Figs. 7 and 8 was out of the scope of the present work.

The results of Figs. 11, 3, and 4 show that the experiments conducted must correspond to kinetic effects of the intracrystalline mass transport of c-C_3H_6 in NaX and not to equilibrium effects alone. The decrease of the flow rate had the effect of bringing the system closer to pseudoequilibrium during the transient (Fig. 11). Therefore, in order to obtain kinetic information about intracrystalline mass transport processes in zeolites using flow reactors, the flow rate should be kept high enough to assure the presence of intracrystalline concentration gradients. On the other hand, by keeping the flow rate low enough so that the transients plotted as in Fig. 11 are not a function of flow rate, equilibrium information could be extracted. Such information has recently been obtained by Hathaway and Davis (*26*) using a semi-batch flow system.

(*B*) *Transient Desorption*

The TPD data of Fig. 12 show that T_m is highest for the lowest coverage of c-C_3H_6 and vice versa. This type of trend may be indicative of a chemisorptive-like interaction (*17*) of c-C_3H_6 which is believed to be due to interaction with the Na^+ cations of the zeolite (*18, 19*). This trend is opposite to that found for encapsulation of H_2 in NaX zeolite (*10*), where T_m is highest for the highest coverage of H_2, but similar to adsorption of NH_3 and hydrocarbons in other zeolite systems (*20, 21*).

For the highest coverage of c-C_3H_6 in these TPD experiments (Fig. 12, curve C) there may also be effects that give rise to an increase in the diffusivity of c-C_3H_6 as a result of an increase in the c-C_3H_6 concentration inside the zeolite cavities. Such effects have been observed for the c-C_3H_6/5A zeolite system (*22*).

The desorption experiment at 70 Torr shows that saturation is rapidly reached after about 5 min. This result indicates that the diffusivity of c-C_3H_6 is affected by the gas phase pressure, which agrees with Darken's relationship for diffusivity (*8*).

The isothermal desorption data of Fig. 13 are important, showing the diffusion effect of c-C_3H_6 leaving the NaX zeolite crystal; it is more pronounced at lower temperatures. For example, reaction of c-C_3H_6 and H_2 with metal-loaded zeolites resulted in residual carbonaceous species (*23*). Accurate estimates of these carbonaceous species by H_2 titration can only be obtained if the zeolite system is first flushed with an inert gas for a period of time consistent with the data of Fig. 13, before a switch to H_2 is made.

The amounts of sorbed c-C_3H_6 determined from the desorption experiment of Fig. 13 are in good agreement with the amounts calculated from the sorption experiments of Fig. 6. The shapes of these transient sorption and desorption curves are markedly affected when Brønsted sites are more abundant than with NaX zeolite (*24*).

The isothermal transients of Figs. 1–6 and 13 can be used to calculate diffusivities, but the time-varying boundary conditions require complete implemented analyses which are the subject of a study in progress. It is appropriate to note here that according to the results of Fig. 3 intercrystalline diffusion need not be accounted for.

CONCLUSIONS

Cyclopropane strongly sorbs in the micropores of NaX zeolite, presumably due to some interaction with Na^+ cations. The results suggest that the apparent diffusivity of c-C_3H_6 is influenced by collisions with diluent gases and by the partial pressure of c-C_3H_6. Diffusion of c-C_3H_6 out of the zeolite in Ar flow is an activated process. Thermodynamic parameters have been determined according to a Langmuir isotherm under appropriate experimental conditions. Transient experiments reported here indicate that c-C_3H_6 does not react with NaX zeolite, and, therefore, are representative of mass transport processes occurring in the microstructure of the zeolite.

APPENDIX

The appropriate material balance equation for the experiments of Fig. 4, in the case where pseudoequilibrium is achieved, is

$$q(C_f - C) = V_i W_z \frac{dC_i}{dt} + V_g \frac{dC}{dt}, \quad (4)$$

where q is the volume flow rate (cm^3/s), C_f is the c-C_3H_6 feed concentration (mol/cm^3), C is the c-C_3H_6 gas phase concentration (mol/cm^3), V_i is the intracrystalline void volume of NaX zeolite (cm^3/g), W_z is the amount of zeolite sample (g), C_i is the c-C_3H_6 concentration in the zeolite cavities (mol/cm^3), V_g is the gas phase volume of the CSTR microreactor (cm^3), and t is the experimental time (s). If at any time t during the transient uptake experiments of Fig. 4 the c-C_3H_6 throughout the zeolite cavities (C_i) is in equilibrium with the c-C_3H_6 outside the zeolite crystal (C) governed by a Langmuir isotherm relationship,

$$\frac{C_i}{C_i^{sat}} = \frac{bCRT}{1 + bCRT} \quad (5)$$

then Eq. (4) can be rearranged to give

$$\frac{dZ}{dv} = \frac{1 - Z}{\left(\frac{V_i W_z C_i^{sat} bRT}{(1 + bRTC_f Z)^2} + V_g\right)}. \quad (6)$$

Here, C_i^{sat} is the c-C_3H_6 concentration inside the zeolite cavities at saturation (mol/cm^3), $Z = C/C_f$ is a dimensionless concentration, and $v = qt$ is the independent variable. Equation (6) can be solved exactly, and the result obtained is shown in Fig. 11. The following experimental values have been used: $V_i = 0.204$ (cm^3/g), $W_z = 0.018$ (g), $C_i^{sat} = 8.63 \times 10^{-3}$ (mol/cm^3), $b = 1.25$ (Torr^{-1}), $T = 313$ K, $C_f = 1.95 \times 10^{-7}$ (mol/cm^3), $V_g = 0.75$ (cm^3). The values of b and C_i^{sat} are based on the data at 2.0 and 3.8 Torr. In addition, V_i represents the void volume of supercages (α cages) of NaX, where c-C_3H_6 is most likely to be found.

ACKNOWLEDGMENTS

The support of the Department of Energy, Office of Basic Energy Sciences, Division of Chemical Sciences is gratefully acknowledged. We thank Dr. Lloyd Abrams of E.I. DuPont for helpful discussions.

REFERENCES

1. Bennett, C. O., *in* "Catalysis Under Transient Conditions" (A. T. Bell and L. L. Hegedus, Eds.), ACS Symposium Series, Vol. 178, p. 1. Am. Chem. Soc., Washington, DC, 1982.
2. Happel, J., "Isotopic Assessment of Heterogeneous Catalysis." Academic Press, New York, 1986.
3. Efstathiou, A. M., and Bennett, C. O., *J. Catal.* **120,** 118 (1989), and references cited therein.
4. Efstathiou, A. M., and Bennett, C. O., *J. Catal.* **120,** 137 (1989), and references cited therein.
5. Stockwell, D. M., Chung, J. S., and Bennett, C. O., *J. Catal.* **112,** 135 (1988).
6. Stockwell, D. M., and Bennett, C. O., *J. Catal.* **110,** 354 (1988), and references cited therein.
7. Nwalor, J. U., Goodwin, J. G., Jr., and Biloen, P., *J. Catal.* **117,** 121 (1989), and references cited therein.
8. Ruthven, D. M., "Principles of Adsorption and Adsorption Processes." Wiley, New York, 1984.
9. Suib, S. L., and Zhang, Z., ACS Symp. Ser. **368,** 569 (1988).
10. Efstathiou, A. M., Suib, S. L., and Bennett, C. O., *J. Catal.* **123,** 456 (1990).
11. Breck, D. W., "Zeolite Molecular Sieves." Wiley, New York, 1974.
12. Neddenriep, R. J., *J. Colloid Interface Sci.* **28,** 293 (1968).
13. Breck, D. W., *J. Chem. Educ.* **41**(12), 678 (1964).
14. Barrer, R. M., and Petropoulos, J. H., *Surf. Sci.* **3,** 126 (1965).
15. Kärger, J., Zikanova, Z., and Kocirik, M., *Z. Phys. Chem. Leipzig* **265,** 587 (1984).

16. Sajkowski, D. J., Lee, J. Y., Schwank, J., Tian, Y., and Goodwin, J. G., Jr., *J. Catal.* **97,** 549 (1986).
17. Efstathiou, A. M., and Bennett, C. O., *J. Catal.* **124,** 116 (1990).
18. Zakharieva-Pencheva, O., Forster, H., and Seebode, J., *J. Chem. Soc. Faraday Trans. 1* **82,** 3401 (1986).
19. Klier, K., *Adv. Chem. Ser.* **101,** 480 (1971).
20. Choudhary, V. R., Srinivasan, K. R., and Akolekar, D. B., *Zeolites* **9,** 115 (1989).
21. Forni, L., Magni, E., Ortoleva, E., Monaci, R., and Solinas, V., *J. Catal.* **112,** 444 (1988).
22. Ruthven, D. M., Loughlin, K. F., and Derrah, R. I., "Molecular Sieves," Advances Chem. Ser., Vol. 121, pp. 330–344. Am. Chem. Soc., Washington, DC, 1973.
23. Schwank, J., Lee, J. Y., and Goodwin, J. G., Jr., *J. Catal.* **108,** 495 (1987).
24. Efstathiou, A. M., Suib, S. L., and Bennett, C. O., submitted for publication.
25. Wu, J. C. S., Goodwin, J. G., Jr., and Davis, M., *J. Catal.* **125,** 488 (1990).
26. Hathaway, P. E., and Davis, M. E., *Catal. Lett.* **5,** 333 (1990).